In-Beam Fast-Timing Technique for Nuclear Structure Studies

S. Lalkovski

27 February 2013

Overview

Definitions

- **Decay modes:** α, β, γ, fission, proton emission, neutron emission etc.;
- **Radioactive decay low:** $A = A_0 \exp^{-\lambda t}$, where
  - λ is the decay constant
  - $\tau = 1/\lambda$ is the mean lifetime
  - $T_{1/2} = \ln 2 \times \tau$ is the half-life
  - $\lambda = \sum_i \lambda_i$, where λ_i is the partial decay constant
- **Typical time range:** 45 orders of magnitude;
  Extremes: ^{1}H, stable
  - $A = 294$, $Z = 117$, $T_{1/2} = 0.08$ s
  - ^{50}V, EC, $T_{1/2} > 2.1 \times 10^{17}$ y.;
  - ^{8}Be, ground state:
    $T_{1/2} = 1.4 \times 10^{-19}$ s;
    first excited state:
    $T_{1/2} = 7.1 \times 10^{-22}$ s.

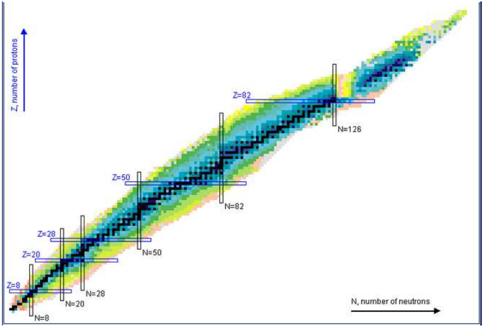

Overview

Definitions

- **Decay modes:** α, β, γ, fission, proton emission, neutron emission etc.;
- **Radioactive decay low:** $A = A_0 \exp^{-\lambda t}$, where
  λ is the decay constant
  $\tau = 1/\lambda$ is the mean lifetime
  $T_{1/2} = \ln 2 \times \tau$ is the half-life
  $\lambda = \sum_i \lambda_i$, where λ_i is the partial decay constant
- **Typical time range:** 45 orders of magnitude;
  Extremes: ^{1}H, stable
  $A = 294$, $Z = 117$, $T_{1/2} = 0.08$ s
  ^{50}V, EC, $T_{1/2} > 2.1 \times 10^{17}$ y.;
  ^{8}Be, ground state:
  $T_{1/2} = 1.4 \times 10^{-19}$ s;
  first excited state:
  $T_{1/2} = 7.1 \times 10^{-22}$ s.

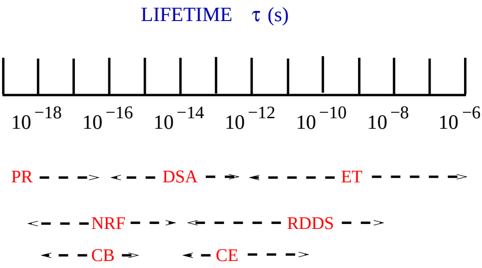

Methods

- **PR** Proton Resonances
- **DSA** Doppler Shift Attenuation
- **ET** Electronic timing
- **NRF** Nuclear Resonance Fluorescence
- **RDDS** Recoil Distance Doppler Shift
- **CB** Channel blocking
- **CE** Coulomb excitation

Fast-slow coincidence circuit

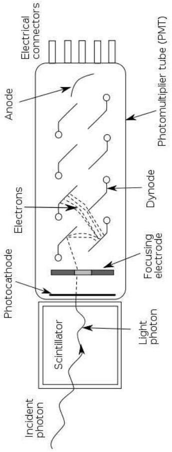

Method

The coincidence circuit measures the distribution of the delayed time signals formed by the "start-stop" TAC time difference.

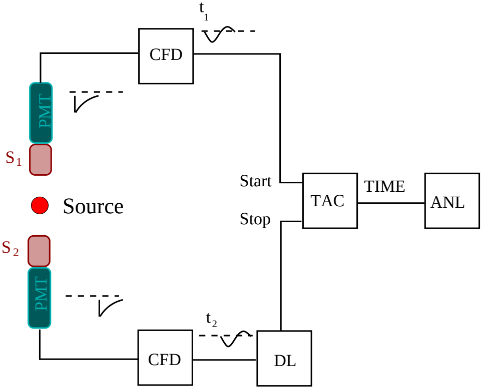

Pulse signals

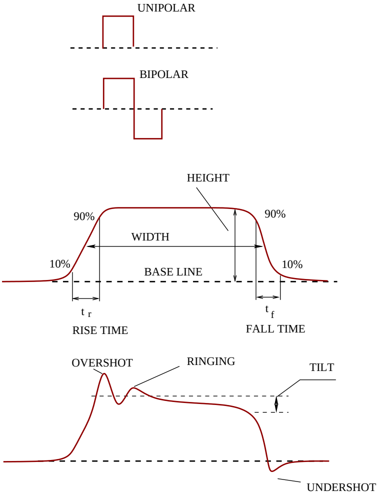

Definitions

- **Baseline:** The BL of the signal is the voltage/current to which the pulse decays.
- **Pulse height or Amplitude:** The Amplitude is the height of the pulse as measured from the maximum value to the baseline.
- **Signal width:** SW is usually measured by the FWHM.
- **Leading Edge:** The LE is the flank of the signal which comes first in time.
- **Rise time:** The time that takes for the pulse to rise from 10% to 90% of its full amplitude.
- **Falling edge or Tail:** The FE is the flank which comes last in time.
- **Fall time:** The time it takes to the signal to fall from 90% to 10% of its amplitude.
- **Unipolar pulse:** The pulse is on one side of the baseline, forming only one major lob.
- **Bipolar pulse:** The bipolar pulse crosses the baseline forming a second major lob on the opposite side of the baseline.

Timing technique

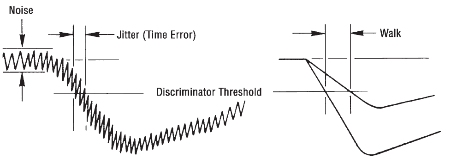

Fig. 1. Jitter and Walk in Leading-Edge Time Derivation.

Leading Edge Discriminator

LED incorporates a voltage comparator with a threshold, which can be set to a given voltage. When the leading edge of the analog pulse crosses this threshold the comparator generates a logic pulse. The logic pulse ends when the trailing edge of the analog pulse crosses the threshold in the opposite direction. The initial transition of the logic pulse is used to mark the arrival time of the analog pulse.

Main Timing Constrains

The jitter is caused by the electronic noise, superimposed on the analogue signal. The jitter depends on the photons generation rate in the crystal, variations in the photon transit time in the crystal, variations of the photo-electron transit time from the cathode to the first dynode, statistical fluctuations in the gain of the individual dynodes;
The walk effect is caused by the time dependence on the amplitude of the signal, i.e. signals with different amplitudes cross the threshold in different moments;

Timing technique

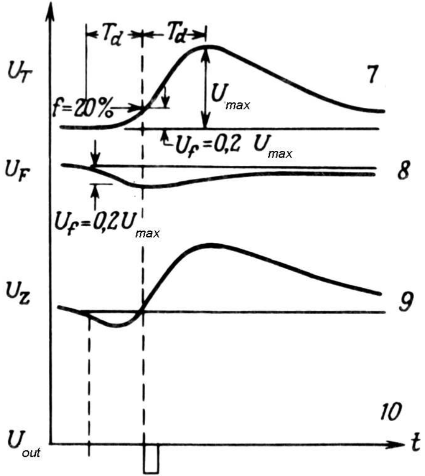

Constant Fraction Discriminator

The input signal is split into two parts. One part is attenuated to a fraction f of the original amplitude, and the other part is delayed and inverted. These two signals are subsequently added to form the constant-fraction timing signal. The method reduces significantly the walk, caused by the amplitude dependence.

The walk and the jitter are minimized by proper adjustment of the zero-crossing reference, and by selection of the correct attenuation factor and delay.

CFD Walk adjustment

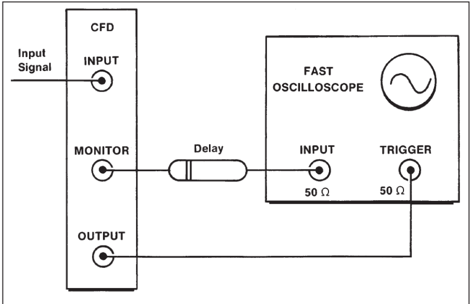

Fig. 11. System Interconnection to View Walk Adjustment.

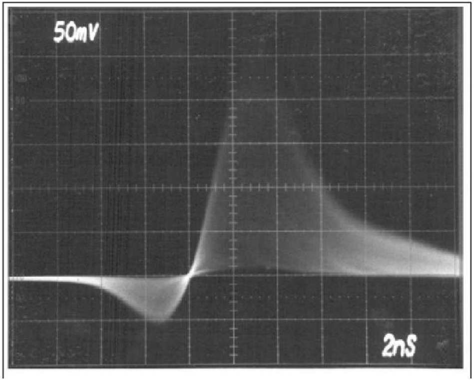

Time-to-amplitude converter

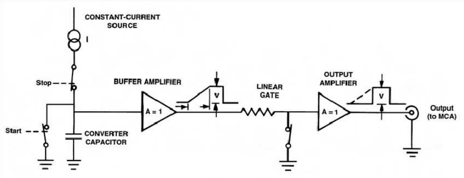

Fig. 1. A Functional Diagram of a Time-to-Amplitude Converter.

• The CFD "start" signal opens the "start" switch. The capacitor begins to charge.
• The CFD "stop" signal opens the "stop" switch, which prevents any further charging of the capacitor. Because the charging current I is constant, the voltage developed on the capacitor is given by

$$V = \frac{It}{C},$$

t is the time interval between start and stop pulses. C is the capacitance of the converter capacitor, i.e. **the voltage is proportional to the time interval**.

• The voltage pulse is passed through the buffer amplifier to the linear gate.
• A short time after the stop pulse arrives, the linear gate switch opens to pass the voltage pulse through the output amplifier to the TAC output.
• Few microseconds latter, all switches return to the closed condition, which terminates the output pulse and discharges the capacitor to ground potential.

The result is a rectangular output pulse with a width of a few microseconds and an amplitude that is proportional to the time interval between the start and stop pulses. This pulse is typically fed to an ADC or a multichannel analyzer for pulse-height measurement.

Fast-slow coincidence circuit

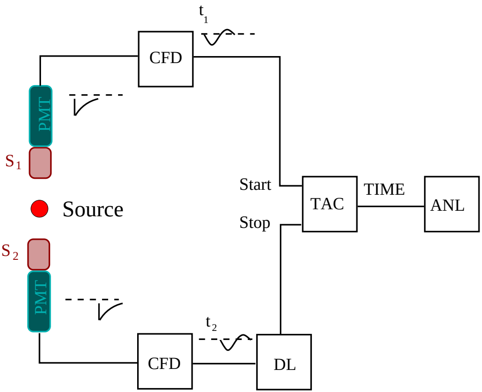

Calibration

- Use of a single PMT do deliver both "start" and "stop" TAC signals.
- Use of a source, which issues "simultaneously" particles and/or gammas.

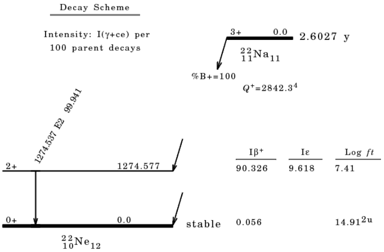

Prompt response function

B.Bengtson and M.Moszýnski, NIM**204** (1982) 129

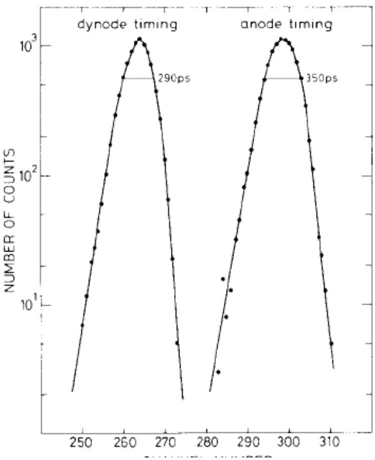

Figure

•**Start:** 1"x1/2" NaI(Tl) coupled to XP2020 PMT
•**Stop:** BIBUQ (organic) scintillator
•**Source:** ^{60}Co
• $\Delta E/E = 20\%$ at 930 keV
• Δt=290 ps from the dynode, 360 ps from the anode

Finite τ

For finite lifetimes τ, the time distribution $F(t)$ of the TAC output signal presents a **convolution** of the PRF with the exponential decay:

$$F(t) = \int \exp(-t'/\tau)P(t-t')dt'/\tau$$

.

Depending on the time range, the lifetime can be evaluated by using • the slope method, when $P(t)/F(t) \ll 1$
• the centroid shift method, when $P(t)/F(t) \gg 1$
• deconvolution, when $P(t)/F(t) \approx 1$

Prompt response function

B.Bengtson and M.Moszýnski, NIM**204** (1982) 129

PRF

The performance of a fast-timing coincidence circuit is characterized by its **prompt response function** $P(t)$, obtained in the limit $\tau \rightarrow 0$.

Optimization

- cooling and polishing;
- optimal geometry: sizes and shapes;
- oil and grease;
- phototube choice;

Year	Scintillator	Phototube	Δt (ps)
Organic scintillators[d]			
1952	Stilbene	1P21	2000
1961	Natlon 136	XP1020	210
1966	Natlon 136	C70045A	185
1970	NE111	XP1021	132
1982	BiBuQ	XP2020	80
Inorganic scintillators[a,d]			
1982	NaI(Tl)	XP2020	290
	CsF	XP2020	150
	BaF_2	XP2020Q	112
1989	BaF_2	R2083Q	101
2010	$LaBr_3$(Ce) 1'×1'	XP20D0B	150
	$LaBr_3$(Ce) 1.5'×1.5'	XP20D0B	180
	$LaBr_3$(Ce) 2'×2'	XP20D0B	300
Semiconductor detectors			
	Ge(Li)[b,d]		5700
	Si[c,e]		180

Table: [a]Dynode pick-up; [b] 35% coaxial detector; [c]surface barrier detector; [d]measured with ^{60}Co source; [e]measured 5.7-MeV α-particles. Plastic scintillator is used as a reference.

$LaBr_3$:Ce

E.V.D. van Loef *et al.*, App.Phys.Lett.**79** (2001) 1573

Properties

- **dopant:** Ce^{3+}, 0.5%
- **PMT:** Hamamatsu R1791
- **Emission wavelenght:** Peaks at 356 and 387 nm
- **Light output:** 61 000(5000) photons/MeV for 662-keV
- **Decay time:** 90% of the emitted light decays with a decay time of 35 ns.
- **Energy resolution:** 2.85(5)
- **Time resolution:** 385 ps. Measured against BaF_2 detector

.

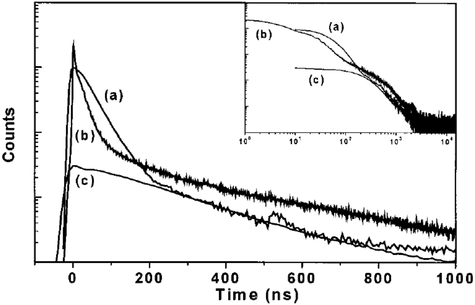

Decay curves of (a) $LaBr_3$:0.5%Ce^{3+},
(b) $LaCl_3$:10%Ce^{3+} and
(c) NaI:Tl

LaBr$_3$:Ce

E.V.D. van Loef *et al.*, App.Phys.Lett.**79** (2001) 1573

Properties

•**dopant:** Ce^{3+}, 0.5%
•**PMT:** Hamamatsu R1791
•**Emission wavelenght:** Peaks at 356 and 387 nm
•**Light output:** 61 000(5000) photons/MeV for 662-keV
•**Decay time:** 90% of the emitted light decays with a decay time of 35 ns.
•**Energy resolution:** 2.85(5)
•**Time resolution:** 385 ps. Measured against BaF_2 detector
.

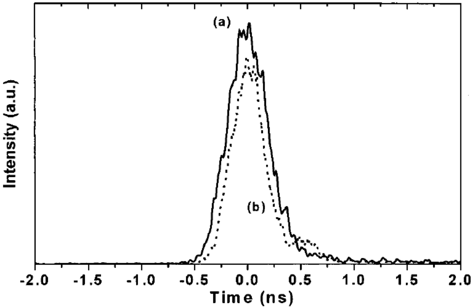

Time resolution of (a) LaBr$_3$:0.5%Ce^{3+} detector and
(b) BaF_2 detector
•**PMT:** XP2020Q
•**Energy threshold:** $E \geq 800$ keV
•**Time resolution:** 385(3) ps

$LaBr_3$:Ce

E.V.D. van Loef *et al.*, App.Phys.Lett.**79** (2001) 1573

Properties

•**dopant:** Ce^{3+}, 0.5%
•**PMT:** Hamamatsu R1791
•**Emission wavelenght:** Peaks at 356 and 387 nm
•**Light output:** 61 000(5000) photons/MeV for 662-keV
•**Decay time:** 90% of the emitted light decays with a decay time of 35 ns.
•**Energy resolution:** 2.85(5)
•**Time resolution:** 385 ps. Measured against BaF_2 detector
.

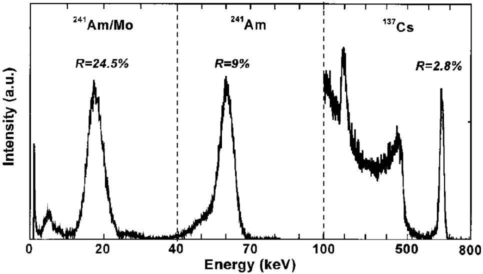

Energy resolution of a single $LaBr_3$:0.5%Ce crystal for x/γ rays from ^{241}Am/Mo, ^{241}Am and ^{137}Cs sources.

Systematics of the ns-isomers.

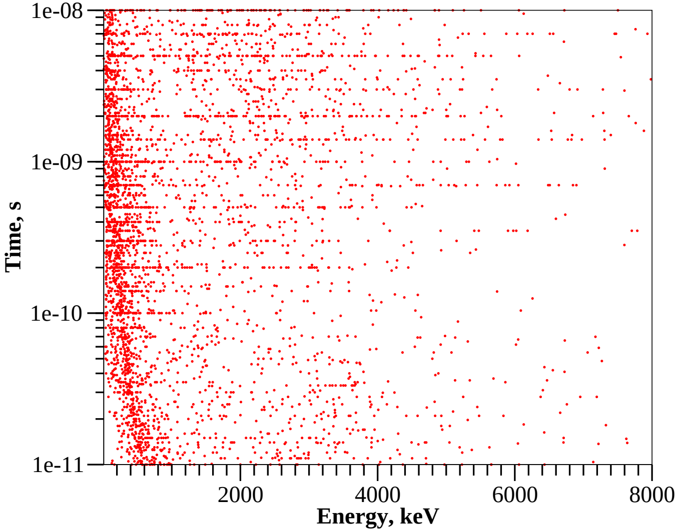

The search is made through out the entire chart of nuclei.

Proton-γ technique

S.Cochavi, J.M.McDonald, and D.B.Fossan, Phys.Rev.**C3** (1971) 1352

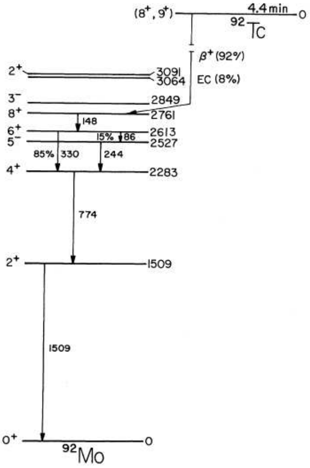

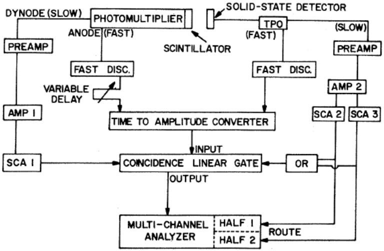

FIG. 4. A schematic diagram of the experimental electronics for the p-γ delayed-coincidence technique.

- **Start:** 1000-μm silicon detector, gated on the 5^-_1 proton group
- **Stop:** $1\frac{1}{2}$-in$\times1\frac{1}{2}$-in NaI, gated on 244-keV γ-rays

Proton-γ technique

S.Cochavi, J.M.McDonald, and D.B.Fossan, Phys.Rev.**C3** (1971) 1352

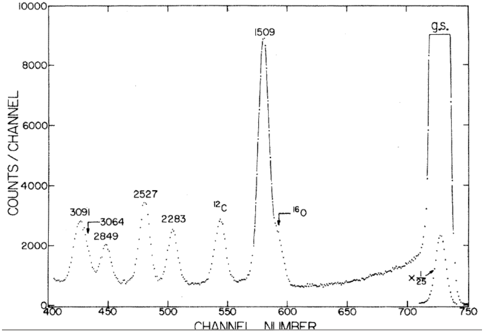

Proton spectrum from $^{92}Mo(p,p'\gamma)$ reaction.

$$T_{kin}(channel) = Q - E^{\star}$$

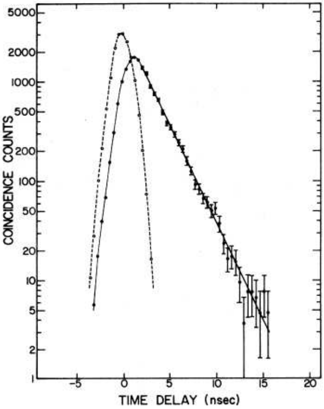

FIG. 5. The experimental decay curve for the 2527-keV 5_1^- state in ^{92}Mo. The decay curve for the 5_1^- state is shown with filled circles and the solid line. The right slope of the decay curve corresponds to a mean life $\tau = 2.24 \pm 0.06$ nsec. The open circles represent the prompt-resolution function.

$\beta - \gamma - \gamma$ coinc.

H.Mach, R.L.Gill and M.Moszyński, NIM**A280** (1989) 49

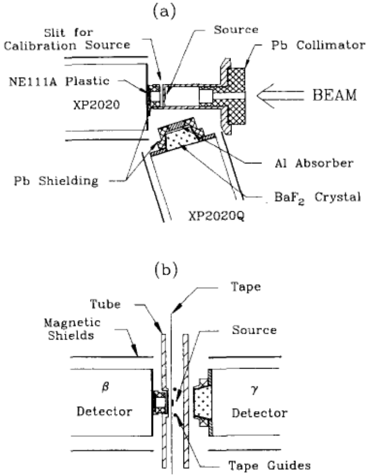

Detectors

- one 3 mm thin NE111A plastic scintillator, coupled to XP2020 PMT, and mounted at 4-7 mm from the source.
- one conical BaF_2 crystal with $\phi = 2.5$ and 1.9 cm and $h = 1.3$ cm, coupled to XP2020 PMT.
- two HPGe detectors, placed 5-7 cm from the source.

$\beta - \gamma - \gamma$ coinc.

H.Mach, R.L.Gill and M.Moszyński, NIM**A280** (1989) 49

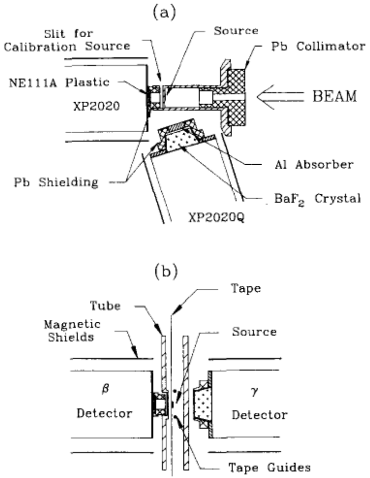

Geometry

• (a) Mass-separated source deposited on a 0.3 mm end cap;
Need of Pb collimator and small beam sizes (1-2 mm) since deviations of the beam position with 1-2 mm can result in 3- to 6-ps shifts in the centroid.
The detector is shielded from the conversion electrons ($E \approx 500$ keV) by a thin aluminum window in the target chamber.
Note: The technique is used for β-decay studies from n-rich nuclei, where $Q_\beta \geq 8$ MeV.
Need of a passive anti-Compton shielding.
• (b) The activity is deposited on a 1.3 cm thick Mylar tape, 50 cm from the detectors set up;
After a pre-determined collection time, the tape moves and the activity is delivered to the detectors area;
Needed a careful shielding is needed to suppress Compton scattering

$\beta - \gamma - \gamma$ coinc.: Electronics

H.Mach, R.L.Gill and M.Moszyński, NIM**A280** (1989) 49

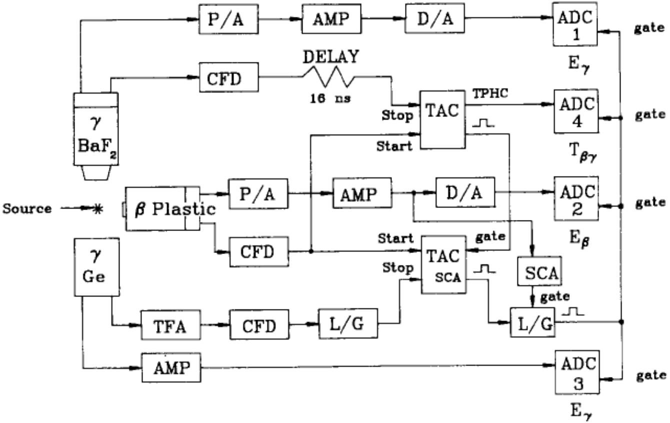

$\beta - \gamma - \gamma$ coincidences

H.Mach, R.L.Gill and M.Moszyński, NIM**A280** (1989) 49

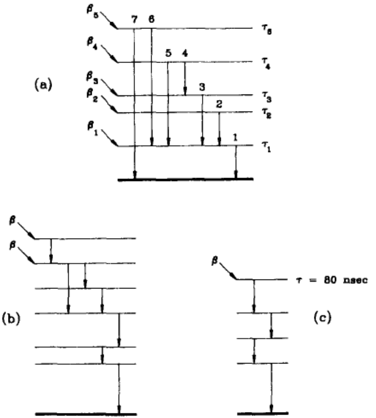

Fig. 1. General features of a decay scheme following the decay of a β-emitter of low spin (a) and high spin (b) and (c). See the text for details.

The time distribution **centroid** position is
$\tilde{t} = \sum_j f_j t_j / \sum_i f_i$,
where t_i is the time channel and f_j is the number of counts in the channel j.

A relative comparison: sequential transitions

- If γ_1 is detected by the Ge detector (HPGe) and γ_2 – by the fast-timing detector (FTD), while β_2 by the β detector (BT), then the time delay is

$$t_1 = \tau_0 + \tau_2 \ ,$$

where τ_0 is the PRF position and τ_2 is the mean lifetime (MNLT) for level "2".

- If γ_2 is detected by the HPGe and γ_1 – by the FTD, while β_2 by the BT detected by the, then the time delay is
$t_2 = \tau_0 + \tau_1 + \tau_2$,
where τ_1 is the MNLT of level "1":
$\tau_1 = t_2 - t_1$.

$\beta - \gamma - \gamma$ coincidences

H.Mach, R.L.Gill and M.Moszyński, NIM**A280** (1989) 49

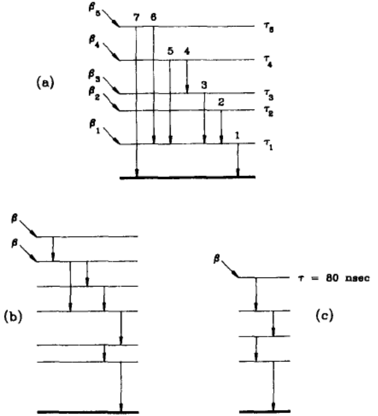

Fig. 1. General features of a decay scheme following the decay of a β-emitter of low spin (a) and high spin (b) and (c). See the text for details.

A relative comparison: parallel transitions

- If γ_4 in HPGe, γ_1 in FTD and β_4 in BD, then $t_4 = \tau_0 + \tau_1 + \tau_3 + \tau_4$.
- If γ_5 in HPGe, γ_1 in FTD and β_4 in BD, then $t_5 = \tau_0 + \tau_1 + \tau_4$, and the MLT of level "3" is $\tau_3 = t_4 - t_5$

Absolute comparison

- If τ_2 is known, the equation $t_1 = \tau_0 + \tau_2$ can be used to determine PRF position. Then, the MLT for each level can be calculated.

$\beta-\gamma-\gamma$ coinc.: Example

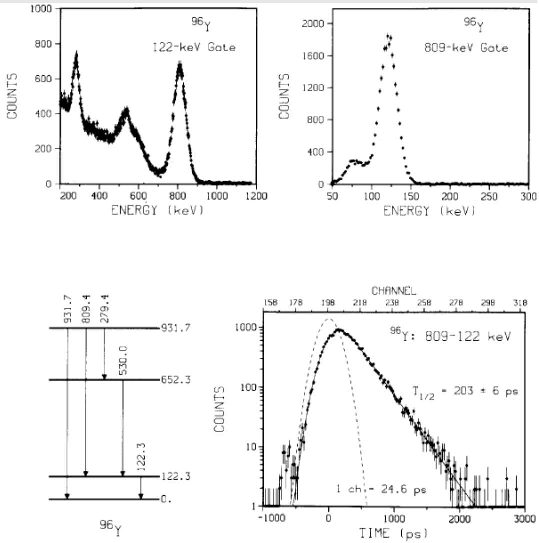

H.Mach, R.L.Gill and M.Moszyński, NIM**A280** (1989) 49

(up) BaF_2 energy spectra, gated on 122-keV and 809-keV transitions with HPGe

(down,left) Partial level scheme of ^{96}Y

(down, right) Deconvoluted time distribution, gated on 122-keV and 809-keV transitions.

In-beam $\gamma - \gamma$ coincidences

W.Andrejtscheff, M.Senba, N.Tsoupas, Z.Z.Ding, NIM**A204** (1982) 123

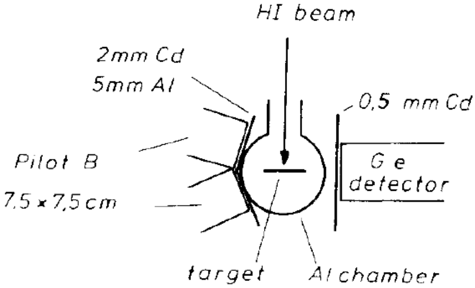

Production

• Excited states, populated in HI reactions with ^{16}O and ^{12}C beams.

Detectors

• two 7.5×7.5 cm Pilot B plastic scintillator, providing "start" TAC signal
or use a beam pulsing system for "start" and
• one 10-ccm planar HPGe, providing "stop" TAC signal
or • a coaxial Ge(Li) detector, providing "stop" TAC signal

Electronics

• Leading Edge Discriminator with a threshold set at $E_\gamma \approx 150$ keV for the plastic scintillator and $E_\gamma \approx$80-150 keV for the Ge detectors.
• Time-to-Amplitude converter

In-beam $\gamma - \gamma$ coincidences

W.Andrejtscheff, M.Senba, N.Tsoupas, Z.Z.Ding, NIM**A204** (1982) 123

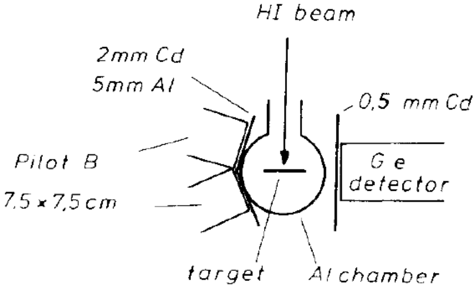

Problems

• several channels open, i.e. $p2n$, $3n$, $\alpha 2n$, αn, pn, $2n$ etc.

• 3-4 statistical γ rays and a number of discrete coincident γ rays.

$T(E_\gamma)$ dependence due to the walk effect.

In-beam $\gamma - \gamma$ coincidences

W.Andrejtscheff, M.Senba, N.Tsoupas, Z.Z.Ding, NIM**A204** (1982) 123

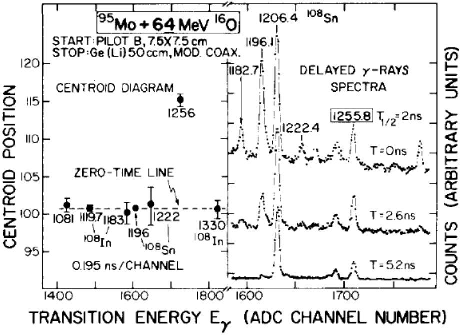

Fig. 3. Prompt and delayed γ-ray spectra as well as the centroid diagram demonstrating the lifetime of the 1256 keV level in ^{109}Sn as $T_{1/2} = 2.0 \pm 0.3$ ns.

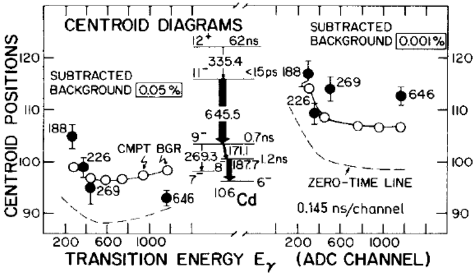

Fig. 4. Partial level scheme [14] and centroid diagrams concerning the lifetimes of the ^{106}Cd levels at 3679 keV (9^-) and 3508 keV (8^-). The time background subtracted per channel from each time curve amounts to 0.05% and 0.001% from the total number of counts, respectively (see also fig. 2).

How we produce excited nuclear states?

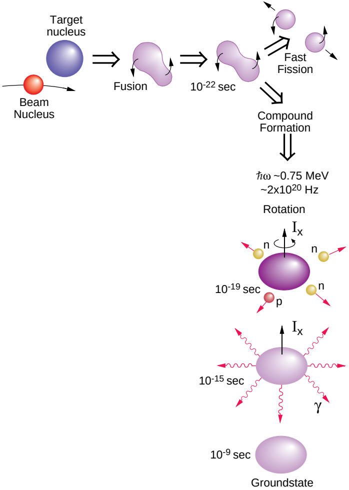

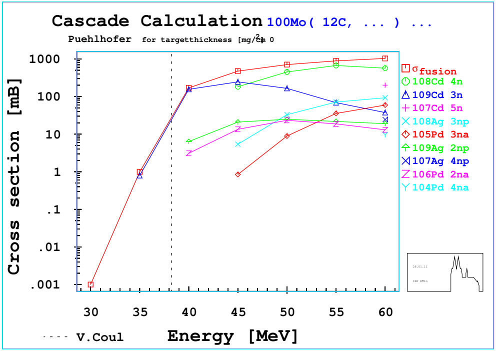

Ion sources: sputtering source

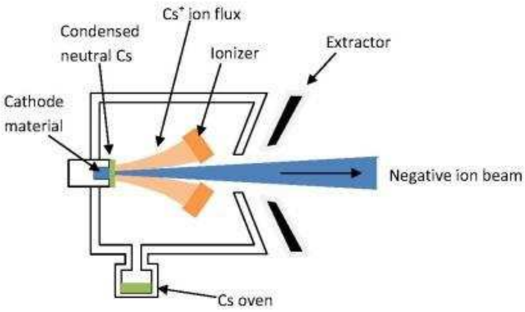

- Cs ions are evaporated from the oven, heated to 1000°
- part of the Cs ions condensate on the cathode, others are positively ionized by the ionizer
- the ionized Cs atoms are accelerated by the negative potential (6 kV) on the cathode, sputtering atoms from the cathode material
- by passing through the condensed cesium atoms on the cathode surface, the sputtered atoms capture an electron and become negatively charged ions
- the negative ions are accelerated away by the negative cathode potential and extracted through the positively charged (12 kV) extractor
- the beam is pre-accelerated in a 50-kV potential and injected into the accelerator, after being analyzed with a bipolar magnet

Accelerator: 9 MV Tandem accelerator

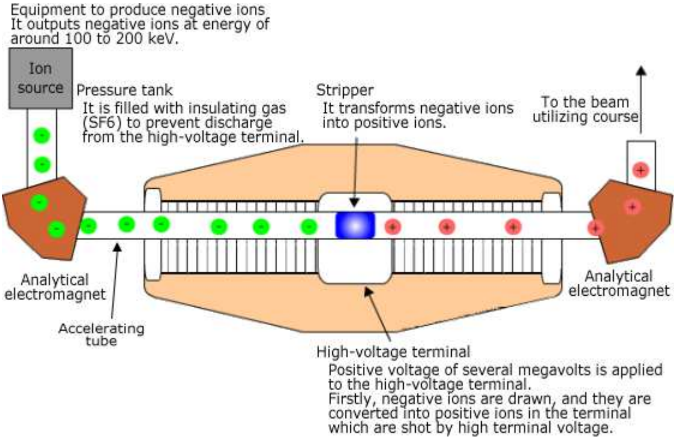

- **stripper:** 5-10 mg/cm^2 carbon foils
- **kinematics** $E = (q+1)V$
  E - kinetic energy in MeV
  V - terminal voltage in MV
  q - charge
- **analyzing magnet:** A/q

In-beam $\gamma - \gamma - \gamma$ coincidences

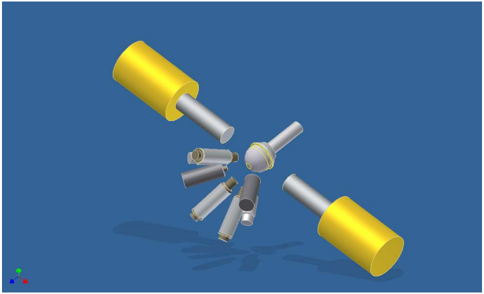

detectors

• two 1-in×1-in cylindrical $LaBr_3$:Ce, mounted on a XP20DOB PMT and placed on forward angles.
• two 1.5-in×1.5-in cylindrical $LaBr_3$:Ce, mounted on a XP20DOB PMT placed on forward angles.
• one 2-in×2-in cylindrical $LaBr_3$:Ce, mounted on a XP20DOB PMT placed on a forward angle.
• two HPGe detectors, placed on 90° with respect to the beam axis.

RoSphere

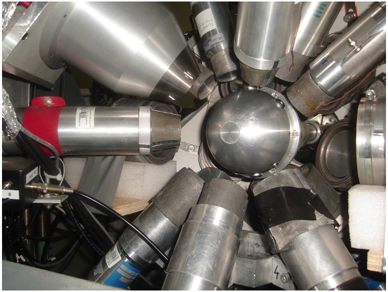

detectors

- 14 HPGe detectors with active Compton suppression
- 11 $LaBr_3$:Ce detectors with passive Compton suppression

Shielded HPGe detector

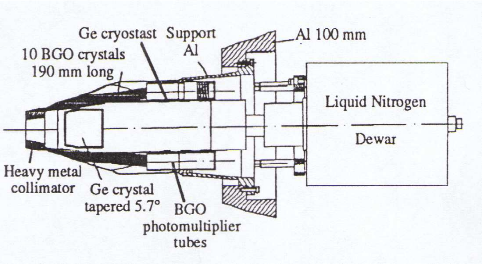

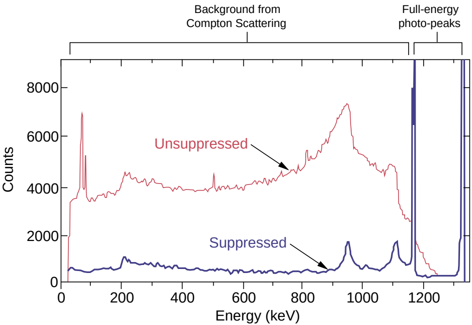

- HPGe detector
- BGO scintillator for shielding
- W collimator
- anti-coincidences between the BGO and HPGe

- Improved peak-to-background ratio (P/B)

In-beam $\gamma - \gamma - \gamma$ coincidences

N.Marginean *et al.*, EPJ**A46** (2010) 329

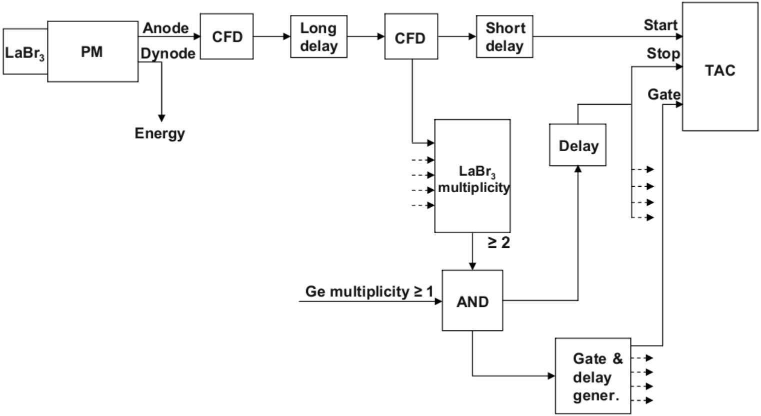

In-beam $\gamma - \gamma - \gamma$ coincidences

N.Marginean *et al.*, EPJ**A46** (2010) 329

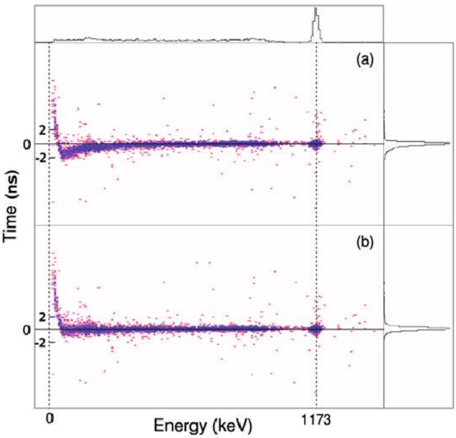

walk correction procedure

• ^{60}Co source placed inside the target chamber; • one of the LaBr$_3$:Ce detectors is chosen as a reference detector. • for each i of the rest of the detectors $E_{\gamma,i}\Delta T_i$ gated matrix is constructed, where ΔT is a time, relative to the reference detector. The gate is on 1332-keV peak in the reference detector. • Polynomial fit to $T(E - \gamma)$ dependence.

Time resolution

- $\approx$ 150 ps for 1-in detector
- $\approx$ 180 ps for 1.5-in detector
- $\approx$ 300 ps for 2-in detector

In-beam $\gamma - \gamma - \gamma$ coincidences

N.Marginean *et al.*, EPJ**A46** (2010) 329

test case

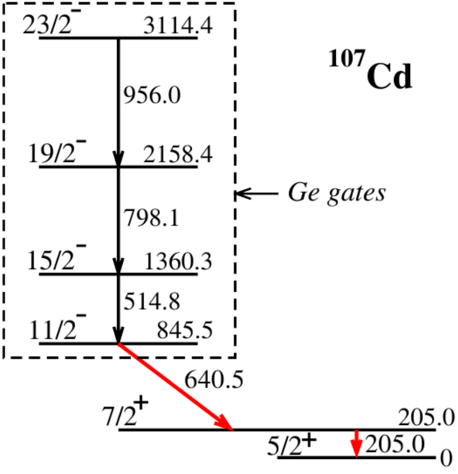

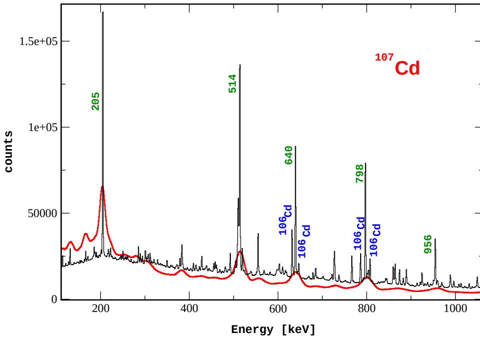

In-beam $\gamma - \gamma - \gamma$ coincidences

N.Marginean *et al.*, EPJ**A46** (2010) 329

test case

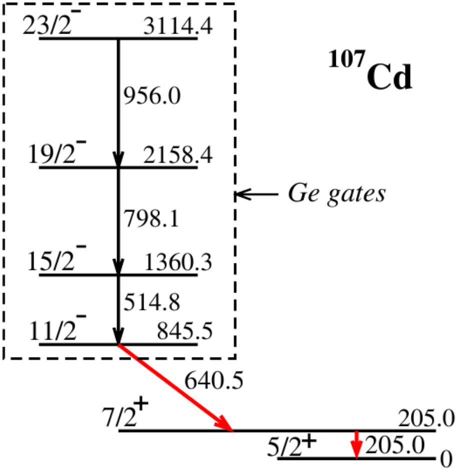

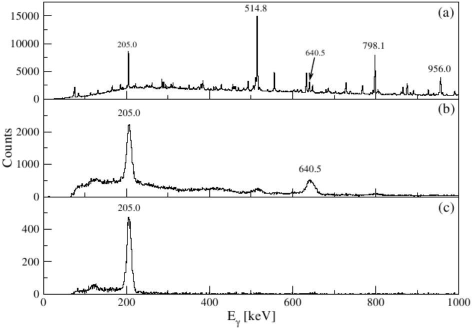

In-beam $\gamma - \gamma - \gamma$ coincidences

N.Marginean *et al.*, EPJ**A46** (2010) 329

test case

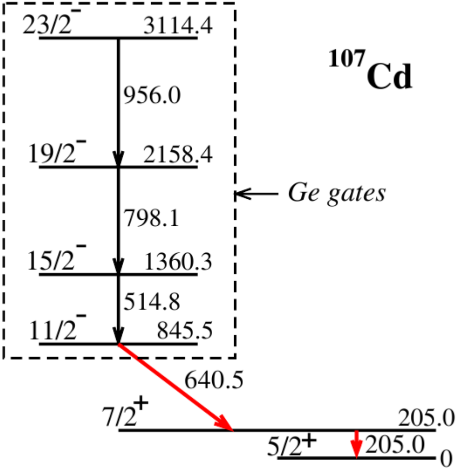

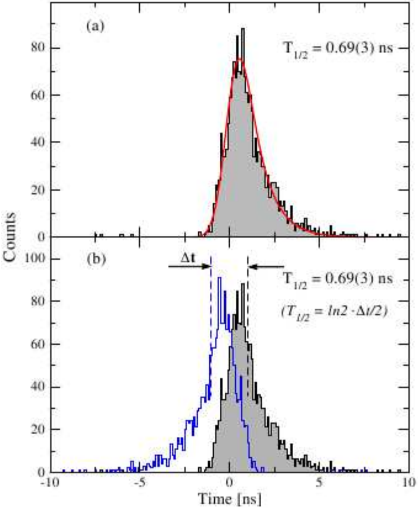

In-beam $\gamma - \gamma - \gamma$ coincidences

N.Marginean *et al.*, EPJ**A46** (2010) 329

^{199}Tl

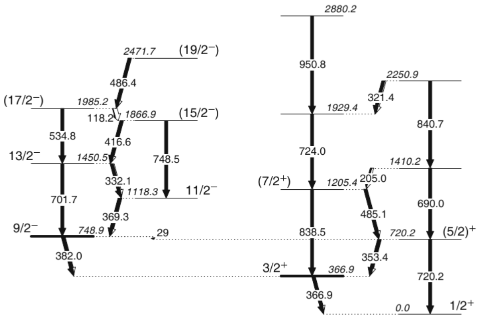

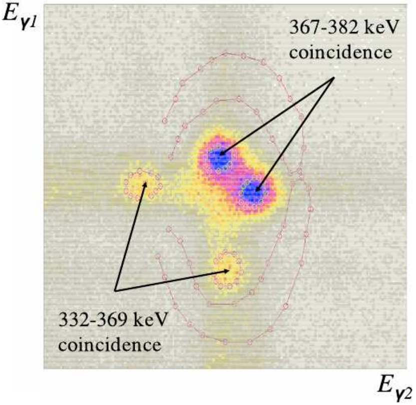

In-beam $\gamma - \gamma - \gamma$ coincidences

N.Marginean *et al.*, EPJ**A46** (2010) 329

^{199}Tl